Generating Electrical Impedance Tomographic Images from Electrical Phantoms in PSpice Circuit Simulator

Jerod Monteiro[1*] and *Pedro* Bertemes[1**]

[1]Santa Catarina State University, Electrical Department, 89219-710 Joinville, SC, Brasil

Abstract. Electrical Impedance Tomography (EIT) is an imaging technique that reconstructs the conductivity of biological tissues based on their electrical properties. The objective is to develop and validate, by PSpice simulations and image reconstructions by EIDORS, the mimicking electrical response of a biological material using 2,224 electrical components. It is built two different electrical phantoms by representing 32 electrodes. An injecting current of 35 mA across a pair of resistors at the edge of the phantom was used. A resistive phantom used resistors of 180 Ω for the mesh, and 128 resistors of 18 Ω to model low resistances areas, whereas 1.8 kΩ for high ones. The second phantom used 128 RC circuit elements of 1.8 kΩ (R) in parallel to 85 nF (C) to simulate an AC excitation from 1 to 100 kHz. The electrical phantoms represent both the mesh's sensitivity to local conductivity variations and the edemas frequency-dependent behavior. The simulations were carried out using PSpice simulations, with image reconstruction performed in MATLAB and EIDORS. By visual inspections, the results indicated that the mesh responded adequately to the resistance change imposed to a particular area of the phantom in the frequency range from 1 to 100 kHz. It can be concluded that an electrical phantom model in SPICE simulator can mimic the tissue property variations, leading to an image of conductivity generated by software EIDORS.

1 Introduction

Electrical Impedance Tomography (EIT) is an imaging technique that reconstructs the conductivity of the human body based on the impedance characteristics of biological tissue [1]. This technique involves injecting current through pairs of electrodes placed on a body surface. Simultaneously, voltage data is collected from the remaining electrodes surrounding this surface. This process is repeated with a frequency sweep, aiming to improve accuracy based on the capacitive response of different biological tissues [2, 3].

Currently, EIT has been primarily applied in clinical contexts, such as lung monitoring, mechanical ventilation control, and the detection of respiratory complications [4].

* Corresponding author: jerod.monteiro@edu.udesc.br
** Corresponding author : pedro.bertemes@udesc.br

Additionally, research has been directed toward its application in neurology and tumor detection [5, 6, 7, 14]. In parallel, the technique has also been explored in industrial applications, such as fault detection in pipelines and quality control in processes involving conductive fluids [8]. In this context, the objective is the development of a segmented and flexible resistive mesh that allows for the controlled parametrization and adjustment of its components, along with a current source system to power the electrodes. Following the validation of the resistive mesh, capacitive edemas will be integrated to observe conductivity variation as a function of frequency.

One of the factors that justify the use of digital simulations is the difficulty in creating biological phantoms that can accurately replicate the physical properties of tissues. In addition, there are limitations regarding the flexibility to alter parameters, and the materials used are subject to wear and degradation over time, affecting the consistency of experiments [9, 10]. Lastly, data collection in these physical models can be compromised, as they are also susceptible to external variables such as temperature and humidity, which tend to cause distortions in measurements, undermining the reliability and reproducibility of biological phantoms.

In contrast, the digital environment, due to its controlled and parameterized nature, allows experiments to be repeated under different conditions without the limitations imposed by biological phantoms. With the validation of the images generated through simulation, it becomes possible to build a consistent and more reliable database [11]. This data can be used to test new methods for solving the inverse problem, which is currently addressed through numerical methods [12, 13].

The main objective of this article is to develop and validate, through PSpice simulations, electrical phantoms capable of simulating the behavior of edema modeled as an RC circuit, aiming to understand the response across different frequencies and generating data for image reconstruction using EIDORS.

2 Methodology

The methodology was divided into the construction of two electrical phantoms and an automated power supply system. Initially, a homogeneous and purely resistive phantom was developed to validate the basic behavior of the mesh under ideal conditions. In parallel, a power supply system was designed based on a current source capable of automatically applying a constant-frequency current to all electrodes in the mesh. In the second stage, a second phantom was built, incorporating capacitive elements to simulate edemas, enabling a multifrequency analysis.

The software tools used to perform the phantom simulations were: i) OrCAD Capture for designing the resistive meshes and the power supply circuit; ii) PSpice A/D for obtaining the simulated data; Stimulus Editor, for generating the digital signals applied to the power supply system; iii) MATLAB for organizing and converting the data into a format compatible with EIDORS; iv) EIDORS itself for data processing and generating the conductivity image of the mesh.

2.1 Resistive Phantom

This involved the modeling of a homogeneous resistive phantom of 32 electrodes. The main objective was to validate the mesh's behavior under ideal conditions. However, limitations within the PSpice simulation environment made it unfeasible to directly construct a single complete mesh. As an alternative, a subgroup containing a reduced mesh was developed and replicated 16 times to contain the final structure.

Each subgroup was structured with an arrangement of resistors along the edges of a square. This configuration allows for a uniform distribution of resistivity. The compatibility of this format with the reconstruction techniques used by EIDORS was also a decisive factor in designing the phantom as it is. Figure 1 shows how each subgroup was developed and how they were connected to the final mesh.

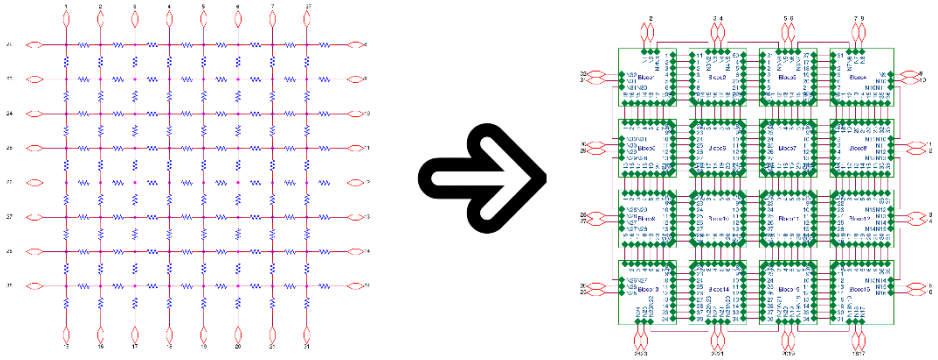

Fig. 1. Mesh of resistors arranged within each subgroup (left). Representation of the connections between each subgroup and the placement of the current injection electrodes (right).

The positioning of the electrodes is also an important factor in order to assure the linearity and reliability of the mesh. Therefore, it was necessary to adjust the angular spacing between the electrodes in order to make it uniform. As a result, the subgroups located in the rightmost column and the last row were modified by adding an extra row of resistor squares to achieve the appropriate angular spacing.

2.2 Automated Power Supply System

The need for a power supply system capable of automatically switching the current source between different pairs of electrodes during the simulation was an important issue to be investigated and addressed in the simulations. Therefore, two pairs of associated multiplexers (1x16) were implemented, one pair was responsible for the positive terminal of the current source and the other for the negative terminal. This configuration enables the sequential selection of current injection pairs, streamlining the simulated data acquisition process. Figure 2 shows the final configuration of the power supply system.

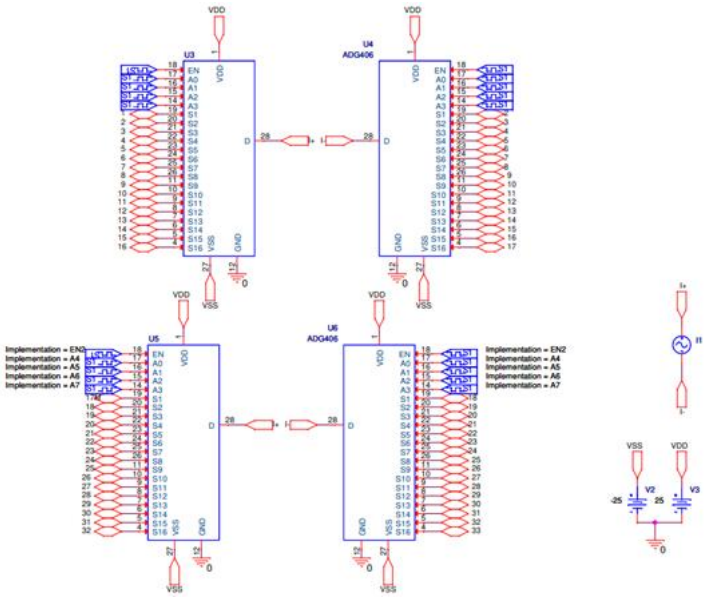

Fig. 2. The final configuration of the power supply system developed in the simulating experiments, where ADG406 is the multiplexer used in the simulations.

The control switches of the multiplexers (A0, A1, A2, A3, and EN) were configured as digital signals derived from successive frequency divisions of the applied current. Each switch followed a division ratio of 1/2, 1/4, 1/8, 1/16 and 1/32, respectively, ensuring that the channel selection occurred sequentially throughout the simulation cycle. This arrangement enabled the automatic scanning of electrode pairs without the need for manual intervention, ensuring greater efficiency during the data collection.

2.3 Multifrequency Phantom

The resistive mesh described above was modified through the insertion of capacitors in order to simulate edemas by varying the impedance as a function of the applied frequency. This adaptation allowed for a more realistic representation of the biological tissues, which exhibit both resistive and capacitive components. Therefore, capacitors were added in parallel with the resistors in the specific cells of the mesh. This configuration enabled the simulation of impedance as a function of frequency, which is essential for multifrequency analysis. Capacitors were strategically placed near the electrodes to increase measurement sensitivity and facilitate the observation of the effects caused by edemas during frequency variation. Figure 3 shows the structure of the mesh with the insertion of capacitors used to simulate capacitive edema. Simulations were conducted for each model. The voltage data obtained were exported to the EIDORS software, which is responsible for reconstructing the conductivity image of the mesh and enabling a visual analysis of the simulated phantom.

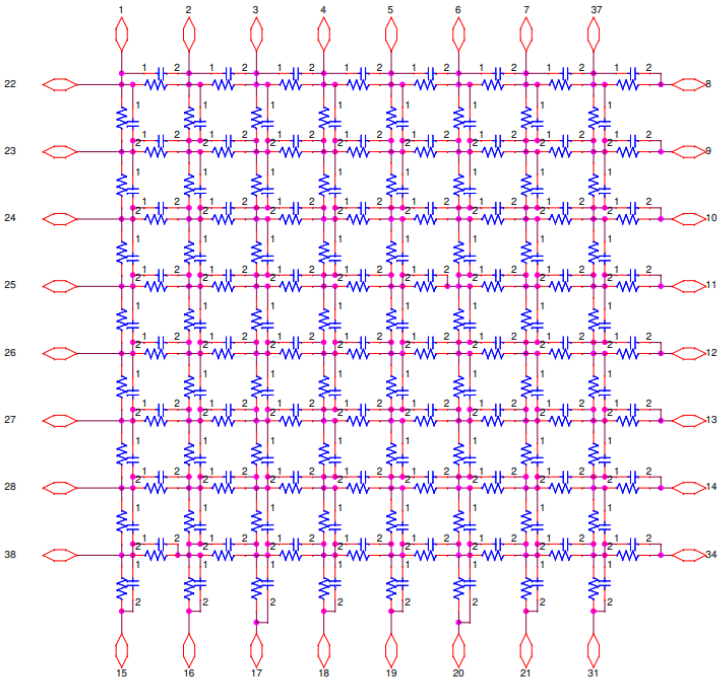

Fig. 3. Schematic diagram of the subgroup with capacitors placed in parallel with resistors in the regions near the electrodes.

3 Results

The simulations were carried out to verify whether the developed phantoms could provide consistent data with the parameters defined during the modelling process. Based on these data, the EIDORS software was used to reconstruct the conductivity images, allowing for an evaluation of whether the generated image matched the expected outcome for each phantom configuration.

3.1 Resistive Phantom

The simulation with the resistive phantom aimed to verify whether the constructed mesh could detect local variations in resistance. To achieve this, a region was parameterized with a resistance 10 times lower than the rest of the mesh, representing an area of low resistance. In a second simulation, the same region was parameterized with a resistance 10 times higher, simulating an area of high resistance. The simulation parameters used were a 180 Ω resistance for the entire homogeneous mesh, to simulate a low-resistance region, a value of 18 Ω was used, while a value of 1.8 kΩ was used to simulate a high-resistance region with a current of 35 mA at 100 kHz was injected for both simulations. Figure 4 shows the images reconstructed by EIDORS based on the simulation data. The closer the color of the pixel is to red, the higher its conductivity. In contrast, the closer the color of the pixel is to blue, the higher its resistivity.

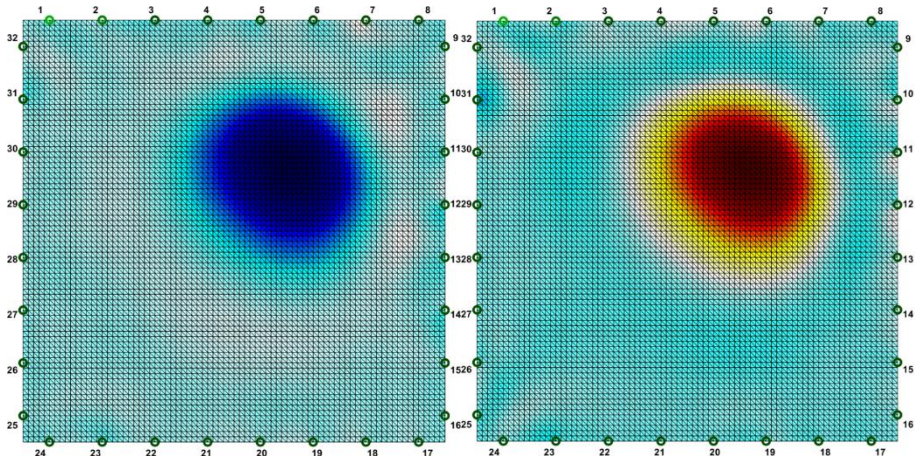

Fig. 4. Image generated of the phantom for a region with resistance ten times lower (right) and higher (left).

It can be observed that the resistive changes were correctly identified, with contrast levels consistent with the applied variations. This result demonstrates that the mesh exhibits good sensitivity to resistance changes, with 6.25% of the electrical phantom corresponding to approximately 16% of the pixels shown.

3.2 Multifrequency Phantom

The objective of the phantom was to investigate the behavior of the conductivity spectra into respect to the addition of capacitive components. It was expected that, as the frequency increased, the region representing the edema would show higher conductivity due to the reduction in capacitive impedance.

The simulation parameters used were a 180 Ω resistance for the entire homogeneous mesh, and 1.8 kΩ for the edema region, simulating a low-resistance area. An 85 nF capacitor was included to model the capacitive properties of the tissue. The current applied during the simulation was 35 mA. Figure 5 shows the variation in conductivity with increasing frequency.

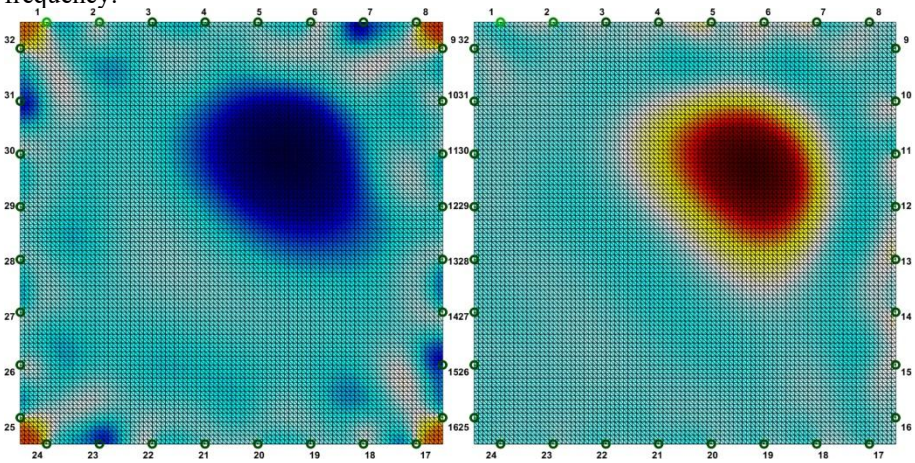

Fig. 5. Conductivity images of the capacitive mesh at 1 kHz and 100 kHz, respectively, from left to right.

It can be observed in Figure 5 that the images generated align with the expected behavior into comparison to the results shown in Figure 4. At low frequencies, the capacitor behaves like an open circuit and then, imposes a little influence on the generated image. As the frequency increases, the capacitive impedance decreases, leading the parallel RC load short-circuiting the resistor R and then, creating an area of high conductivity.

4 Conclusion

The further developments of this technology may lead to greater accuracy and reliability in EIT systems, enabling practical applications in hospital environments. Among the main advantages of this technique compared to other imaging methods are the possibilities of real-time monitoring, non-invasive operation, radiation-free imaging and useful for patients admitted to intensive care units. Additionally, its production cost is significantly lower than a Computed Tomography, for example, but also has the benefit of portability to be used at the patient's bedside.

Simulation showed that the mesh responded as expected to both resistive and capacitive components from DC to 100 kHz. The images generated from the data were consistent with theoretical behavior, indicating that the mesh is also capable of accurately reflecting the changes imposed during simulation parameterization. It can be concluded that an electrical phantom model in SPICE simulator can mimic the tissue property variations, leading to an image of conductivity generated by software EIDORS. The proposed model can also allow adjustments in the electrical circuit for mimicking different types of biological materials. The simulation environment proved to be effective in generating a robust dataset for testing and improving image reconstruction algorithms for EIT systems.

ACKNOWLEDGMENTS

Special thanks to FAPESC (2023TR504) which partially funded this project by means of using the structure of PETBIO-UDESC laboratory for simulations and by the Santa Catarina State University (UDESC) by means of a research scholarship.

References

1. C. Gabriel, S. Gabriel, E. Corthout, The dielectric properties of biological tissues: I. Literature survey, Phys. Med. Biol., 41(11) (1996). https://iopscience.iop.org/article/10.1088/0031-9155/41/11/001
2. S. Mansouri, Y. Alharbi, F. Haddad, S. Chabcoub, A. Alshrouf, A. A. Abd-Elghany, Electrical impedance tomography – recent applications and developments, J. Electr. Bioimpedance, 12(1), 50–62 (2021). https://doi.org/10.2478/joeb-2021-0007
3. B. H. Brown, A. D. Seagar, The Sheffield data collection system, Clin. Phys. Physiol. Meas., 8(4A), 91–97 (1987). https://iopscience.iop.org/article/10.1088/0143-0815/8/4A/012
4. Z. Zhao, F. Fu, I. Frerichs, Thoracic electrical impedance tomography in Chinese hospitals: A review of clinical research and daily applications, Physiol. Meas., 41(4) (2020). https://iopscience.iop.org/article/10.1088/1361-6579/ab81df/meta
5. T. K. Bera, Applications of Electrical Impedance Tomography (EIT): A Short Review, IOP Conf. Ser. Mater. Sci. Eng., 331(1) (2018).

https://iopscience.iop.org/article/10.1088/1757-899X/331/1/012004

6. P. Grasland-Mongrain, C. Lafon, Review on biomedical techniques for imaging electrical impedance, IRBM, 39(4), 243–250 (2018). https://doi.org/10.1016/j.irbm.2018.06.001
7. M. Faulkner, S. Hannan, K. Aristovich, J. Avery, D. Holder, Feasibility of imaging evoked activity throughout the rat brain using electrical impedance tomography, NeuroImage, 178, 1–10 (2018).
   https://doi.org/10.1016/j.neuroimage.2018.05.022
8. Grieve, B. D., Dyakowski, T., Mann, R., & Wang, M. (1999, April). Interfacing of EIT into an industrial pressure filter, A practical example. In Proceedings of 1st World Congress on Industrial Process Tomography (pp. 14-17).
9. Ionita, C. N., Mokin, M., Varble, N., Bednarek, D. R., Xiang, J., Snyder, K. V., Siddiqui, A. H., Levy, E. I., Meng, H., & Rudin, S. (2014). Challenges and limitations of patient-specific vascular phantom fabrication using 3D Polyjet printing. Proceedings of SPIE, 9038, 90380M.
   https://doi.org/10.1117/12.2042266
10. Richardson, C., & Kulkarni, J. (2017). A review of the management of phantom limb pain: challenges and solutions. Journal of Pain Research, 10, 1861–1870. https://doi.org/10.2147/JPR.S124664
11. Clemente, F., Amato, F., Adamo, S., Russo, M., Angelone, F., Ponsiglione, A. M., & Romano, M. (2024). Circuital modelling in muscle tissue impedance measurements. Heliyon, 10(7), e28723.
    https://doi.org/10.1016/j.heliyon.2024.e28723
12. Hrabuska, R., Prauzek, M., Venclikova, M., & Konecny, J. (2018). Image reconstruction for electrical impedance tomography: Experimental comparison of radial basis neural network and Gauss – newton method. IFAC-PapersOnLine, 51(6), 438–443.
    https://doi.org/10.1016/j.ifacol.2018.07.114
13. Menin, O. H. (2009). Método dos elementos de contorno para tomografia de impedância elétrica.
    https://doi.org/10.11606/D.59.2009.TDE-31102009-085546
14. Halter, R. J., Hartov, A., Poplack, S. P., diFlorio-Alexander, R., Wells, W. A., Rosenkranz, K. M., Barth, R. J., Kaufman, P. A., & Paulsen, K. D. (2015). Real-time electrical impedance variations in women with and without breast cancer. IEEE Transactions on Medical Imaging, 34(1), 38–48. https://doi.org/10.1109/TMI.2014.2342719